

**GT2024-121321**

## OPERATION OF FT4000® SINGLE NOZZLE COMBUSTOR WITH HIGH HYDROGEN

**Justin Locke<sup>1</sup>, Wookyung Kim<sup>1</sup>, Lance Smith<sup>1</sup>, Timothy Snyder<sup>2</sup>, James Dayton<sup>3</sup>**

<sup>1</sup>RTX Technology Research Center, East Hartford, CT

<sup>2</sup>Pratt and Whitney, East Hartford, CT

<sup>3</sup>Mitsubishi Power Aero, Glastonbury, CT

### **ABSTRACT**

*This paper reports initial results from an effort to develop a retrofittable fuel/air injector for the FT4000® aeroderivative gas turbine that enables use of hydrogen as a carbon-free fuel for efficient power generation. The FT4000 engine's low-NOx combustor was developed by Pratt & Whitney and RTX Technology Research Center with core technology from the Pratt & Whitney PW4000 turbofan aircraft engine. The work reported here advances the technology readiness level of the FT4000 combustor for operation with hydrogen, starting with an experimental assessment of the current production hardware with increasing hydrogen content mixed with natural gas.*

*High-pressure single-sector combustor rig tests have been completed, demonstrating the ability for the dual fuel nozzle to operate an FT4000 combustor on 100% hydrogen with low nitrogen oxide (NOx) emissions. Metal temperature measurements and video images of the flame structure from zero to 100% hydrogen highlight opportunities to improve the fuel nozzle robustness for high hydrogen conditions.*

*The current FT4000 production engine operates on either natural gas or No. 2 fuel oil with water injection to achieve high thermal efficiency and low emissions. This engine is fielded by Mitsubishi Power Aero and delivers 70 MW of power with a simple-cycle efficiency of over 41% when operating with wet compression. Results from this study have cleared the current production FT4000 engines with dual fuel nozzles to operate at baseload power on blends of hydrogen mixed with natural gas and water.*

**Keywords:** combustion, emissions, gas turbine, hydrogen, power generation, sustainability

### **NOMENCLATURE**

CAEP	Committee on Aviation Environmental Protection
DI	Deionized
FAR	Fuel to air ratio

ID	Inner diameter
JBTS	Jet Burner Test Stand
LBO	Lean blow out
NDIR	Non-dispersive infrared
NG	Natural gas
NOx	Oxides of nitrogen
OD	Outer diameter
P3	Combustor inlet pressure
RQL	Rich quench lean
RTRC	RTX Technology Research Center
SCR	Selective catalytic reduction
SNR	Single nozzle rig
T3	Combustor inlet temperature
T4	Combustor exit temperature
TALON	Technology for Advanced Low NOx
TC	Thermocouple
UHC	Unburned hydrocarbons
WFR	Water to fuel ratio (on mass basis)



**FIGURE 1. FT4000® Aeroderivative Dual Fuel Gas Turbine Engine.**



FIGURE 2. Pratt & Whitney Talon IIB combustor.

## 1. INTRODUCTION

### 1.1 Background & Motivation

Pratt & Whitney, RTX Technology Research Center (RTRC), and Mitsubishi Power Aero LLC developed the aeroderivative FT4000® engine with core technology from the Pratt & Whitney PW4000 turbofan engine. The FT4000 gas turbine engine (Fig. 1) is available in both single and dual-engine configurations and provides dual-fuel capability for operation on natural gas or liquid fuel (No. 2 fuel oil). It offers greater than 41 percent simple-cycle efficiency and a nominal 70 to 140 MW of power within a modular design [1]. The SWIFTPAC® gas turbine package is designed to provide reliable peaking and base load power with a relatively compact footprint. This is accomplished by coupling either one or two FT4000 engines to one electric generator.

The FT4000 combustor design is based on the low emissions aeroengine TALON IIB (Technology for Advanced Low NOx) rich-quench-lean (RQL) combustor (Fig. 2). Like the PW4000, the FT4000 combustor manages the fuel/air mixture stoichiometry in separate combustion zones to minimize the time the mixture spends at high temperatures where NOx is typically generated. The primary zone of the combustor burns a rich mixture of fuel and air. Subsequently, large amounts of “quench” air are introduced and rapidly mixed with the rich products, bringing the average stoichiometry well into the lean range inside the secondary zone where combustion is completed [2]. The FT4000 combustor has optimized the injection of water to manage peak flame temperatures and meet regulatory NOx requirements while maintaining low CO emission levels. One objective of the present study is to determine how much water is required to reduce NOx emissions in a hydrogen-fueled FT4000, to enable low NOx emissions on both natural gas and natural gas/hydrogen blends up to 100% hydrogen.

The FT4000’s high operating pressure ratio of 36 and inlet temperatures up to 1040°F (830K) presents some challenges with respect to the combustion of 100% hydrogen. Hydrogen’s extremely high flame speed and wide flammability limits at these combustor inlet conditions create a significantly higher risk of flameholding than when operating on natural gas or No. 2 fuel oil. Hydrogen flames, with their high flame speeds, wide flammability limits, and short quenching distances, are more

susceptible to anchoring in low-velocity regions like wakes or separation zones. This may even include the wakes downstream of a fuel injection jet or a swirler vane. Therefore, rig testing of the FT4000 combustor configuration with hydrogen fuel is critical to ensuring successful implementation of hydrogen in engine use, whether in natural gas/hydrogen blends or as pure (100%) hydrogen.

Our approach in this work has been to first explore achievable NOx levels with hydrogen fuel in the FT4000’s existing combustor design with water injection, making use of its RQL design and amenability, as a non-premixed combustor, to safe operation on hydrogen. Because RQL combustors mix fuel and air rapidly in the near-field of the fuel injector, rather than within a long premixer, there is little premixing upstream of the intended flame stabilization zone and the risk of flashback and flameholding is reduced. Furthermore, with multiple combustion zones (rich and lean), RQL combustors are less susceptible than lean premixed designs to thermoacoustic instabilities [3] which can arise with changes in fuel, such as from natural gas to hydrogen.

When introducing hydrogen fuel, regardless of whether the combustor design is RQL or purely lean burn, managing the location of combustion remains an important consideration for durability of the fuel/air injector. Flames directly attached to a surface transfer significant heat into the part and can decrease component life. For liquid fuels and natural gas operation, the flames are kept away from the fuel nozzle and uncooled combustor components (such as swirlers) by tailoring the aerodynamic flow field to keep the velocity of the mixture significantly above its turbulent flame speed in these regions. This principally focuses on the avoidance of features that might cause flow separations large enough to hold a flame. For hydrogen, these strategies are more difficult. Hydrogen’s high flame speed and short quenching distance means that even very small low-velocity regions can become areas of concern, with measures being needed to prevent such regions from causing overheating and durability issues in nearby components. In the rig testing reported here, these regions were monitored optically and with metal temperature measurements to evaluate the impact of hydrogen use and mitigation measures on component durability.

### 1.2 Prior Work

As a gas turbine fuel, hydrogen offers many desirable performance characteristics including ease of ignition, robust flame anchoring, high flame speed with rapid burnout for high combustion efficiency, and wide flammability limits for turndown [4-8]. For these reasons hydrogen was used during development of the first aviation jet engine in 1937 [9-10] and was selected to fuel the Model 304 high-altitude reconnaissance-aircraft engine developed by Pratt & Whitney in 1957 [4, 11]. In these early applications, engine NOx emissions were not regulated and were not measured. However, with growing environmental awareness in the 1970s, NASA began investigating NOx emissions from various fuels including hydrogen [13-14]. In the non-premixed combustor designs of

that era, hydrogen was easily substituted for a conventional hydrocarbon fuel with simple fuel injector modification, and the combustor could also be shortened if desired (because of the rapid burnout) [4,12-13], but NOx emissions from these non-premixed systems remained high with hydrogen fuel [13]. By introducing premixing, further investigations of hydrogen combustion for aeroengines at NASA, United Technologies Research Center (now RTRC) / Pratt & Whitney and elsewhere showed significant improvement in NOx emissions but faced persistent challenges with flashback [14-18]. The flashback challenge has also impacted the use of hydrogen fuel for ground power generation, including aeroderivative machines, where development efforts through to the present time have continued to seek low-NOx combustion systems for high-hydrogen fuels [19-29] while having to limit hydrogen levels in fielded systems to avoid flashback and/or high-temperature combustion with concomitant high NOx. It is the same combustion characteristics of hydrogen which provide robust burning that also impose significant challenges for the design of low-NOx combustion systems, exacerbated by extremely wide flammability limits and short quenching distances for hydrogen as compared to hydrocarbons [30-31] that allow hydrogen flames to flashback within the boundary-layer flows of mixers and to anchor on physical features that are only fractions of a millimeter in size. This is a significant challenge to overcome: low-NOx combustion of high-hydrogen fuel is requiring focused investment, experience, and learning before these systems are broadly fielded and available to provide clean power – this current state is perhaps analogous to the state of dry-low NOx combustion systems for natural gas in the 1970s and 80s.

In addition to the pure-hydrogen and high-hydrogen studies cited above, significant effort in recent decades has focused on power generation with hydrogen fuel that is diluted with other components, especially CO (from gasification of carbonaceous fuels) and non-reacting diluents such as N<sub>2</sub>, CO<sub>2</sub>, or H<sub>2</sub>O that are available from syngas-plant processes, as well as with hydrocarbons from refinery-plant streams or biomass sources [32-33]. When diluted sufficiently, flame temperatures for these mixed fuels can be lowered enough to meet NOx emissions regulations (with exhaust gas cleanup by SCR if needed); meanwhile there have also been development efforts toward low-NOx combustor technologies that allow gradually increasing hydrogen levels. Largely with DOE funding, these technologies have been developed and advanced by the major OEM frame-engine manufacturers [20-21, 25, 34-35] and others [36-38]. While these technologies have progressed the state-of-art for low-NOx combustion of high-hydrogen fuels, there remains a gap to achieving low-NOx combustion with 100% hydrogen fuel, or even >50% hydrogen fuel, across a wide range of platforms and particularly in modern, high efficiency, high compression-ratio machines (such as the FT4000).

There is growing commercial demand to close this gap, as power producers seek to site new plants that both meet emissions regulations *and* maximize the use of hydrogen for power production. Operation on 100% hydrogen is desired, as is fuel flexibility. In the changing landscape of 21<sup>st</sup> century energy

production, hydrogen will be used as a zero-carbon fuel for energy storage, energy transport, and power generation from both green and blue hydrogen production sources. The ability to flexibly blend hydrogen into natural gas – varying the proportions according to these fuels' availability – is of particular interest as hydrogen enters the power generation market [39] and will be especially valuable if the percentage of hydrogen can be unconstrained (or at least minimally constrained to high values) so that allowable blends can contain significant energy content in hydrogen. Reaching high levels of hydrogen will be especially challenging in aeroderivative engines because they are generally optimized for high simple-cycle efficiency and consequently have high pressure ratios and high combustor inlet temperatures, making it especially difficult to premix without flashback risk as noted above. The FT4000 engine, for example, is optimized to a world-class 41% simple-cycle efficiency with a pressure ratio of 36 [1,40]. RQL combustors – without premixing and using water injection for NOx control – are one pathway to high-hydrogen fuel use if the change in combustion characteristics due to hydrogen's reactivity can be managed. Under the current study we are addressing these challenges using the RQL approach, in a development program that fully characterizes and then extends the capability of the FT4000 engine to use blends of hydrogen in natural gas with increasing hydrogen content, up to 100%.

## 2. MATERIALS AND METHODS

### 2.1 FT4000 Combustor and Fuel Nozzles

The TALON IIB annular combustor as used in the FT4000 is shown in Fig. 2, oriented with the flow direction from top to bottom. Air enters the combustor through 24 fuel/air injectors inserted through the combustor dome, through an initial first row of quench-air holes located circumferentially around each of the combustor outer (OD) and inner (ID) walls, and through additional dilution air and liner cooling holes. The fuel/air injector (or “fuel nozzle”) is illustrated in Fig. 3. It incorporates two air-swirlers and two fuel circuits that are sandwiched between the two air-swirlers, making it a dual-fuel nozzle with the capability to inject fuel oil and/or water through one circuit and gaseous fuel through the other circuit. A portion of the total combustion air is mixed with the fuel at the nozzle exit, providing a fuel rich mixture in the combustor front-end.

Quench air is added midway through the combustor to complete combustion and dilute the mixture to temperatures suitable for the turbine. While it is referred to as “quench” air, it is more appropriate to call it “secondary combustion air.” The mixture of rich products immediately reacts upon contact with the quench air. With fast mixing, only a fraction of the fuel will burn at or near stoichiometric temperatures. The design of this mixing section is key to the low-NOx performance of the RQL concept. Pratt & Whitney has developed a proprietary approach to designing the mixing holes in relationship to the mixture exiting the fuel nozzle/mixer, and to the flame stabilization zones. These combustor principles are currently employed on the Geared Turbo-Fan family of aero engines [2]. These aero engines produce best-in-class NOx, at approximately

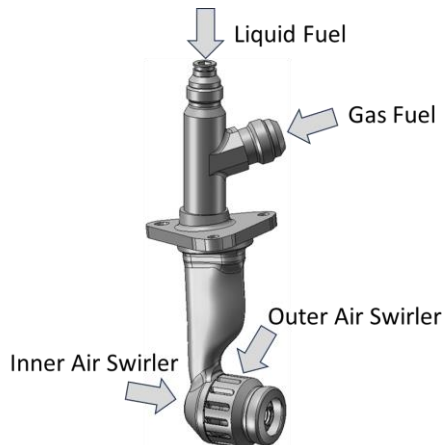


**FIGURE 3. FT4000 production dual-fuel nozzle.**

50% of the Committee on Aviation Environmental Protection (CAEP) standards, CAEP/6 [41].

The FT4000 also employs water injection for further NOx reduction, to meet regulated levels for ground-power installations. Key to success in water injection is to inject it in a manner that leads to the largest reduction in flame temperature without adversely affecting combustion efficiency or operability. As a general guideline, every 70°F reduction in flame temperature decreases NOx production by about half [42]. In the Fig. 3 illustration of the FT4000 fuel nozzle, liquid fuel and water enter via the vertical stem at the top, and then mix with the inner and outer swirler airflow before exiting the fuel injector. Gas fuel enters the fuel nozzle from the stem side and surrounds the liquid fuel passage inside the nozzle. This fuel also mixes with the inner and outer swirler airflow before exiting the fuel injector. Significant effort was expended in development of the FT4000 nozzle to produce a fuel nozzle design that injected the natural gas such that when water was injected in the passages used for the liquid fuel, it decreased the flame temperature uniformly and without impacting combustion efficiency or CO emissions. The design exploration made extensive use of Computational Fluid Dynamics (CFD), which was also used in this study to examine engine (full-annular) versus rig (single-nozzle/single-sector) aerodynamics as well as the impact of hydrogen versus natural gas injection. As discussed below, the single-nozzle rig tests reported here used engine hardware in the combustor front-end, including the fuel nozzle, air swirlers, and air-cooled bulkhead panel or “dome”, to minimize differences between the rig and engine aerodynamics.

## 2.2 Rig Details

These tests were carried out at the RTX Technology Research Center (RTRC)’s Jet Burner Test Stand (JBTS), leveraging existing high-pressure test capability and hydrogen infrastructure. The JBTS facility flowrate capacity for its single sector centerline matches one sector of the 24-sector (24-nozzle) annular combustor in the FT4000 engine, at full engine-pressure conditions. A photograph of RTRC’s single sector centerline is shown in Fig. 4. Testing was performed using one engine fuel

nozzle in a custom-designed single-sector test section closely matching the full-annular combustor aerodynamics. A solid-model cutaway image of the single-sector rig is illustrated in Fig. 5. The components illustrated in red in the figure represent production or “bill-of-materials” engine hardware, while the rig frame and associated components are illustrated in grey to represent hardware that was custom-built for this test campaign. As shown, the rig’s front-end comprises the FT4000 engine fuel nozzles, swirlers, and the air-cooled bulkhead panel, while the remainder of the rig is built to approximate the remaining FT4000 combustor geometry. Components shown in grey are water cooled using a closed-loop water-cooling supply to provide robust operation across a wide range of operating conditions and hydrogen/natural-gas blends. An aft-looking-forward photograph of the as-tested bulkhead panel and fuel-nozzle/swirler assembly is shown in (Fig.6 (a)). Combustor emissions are sampled from holes on centers-of-equal-area in the horizontal tubes traversing the flowpath at the combustor exit. A forward-looking-aft photograph of the closed-loop water-cooled emissions probe is shown in (Fig. 6 (b)).

Because the combustor rig is water cooled aft of the bulkhead, liner cooling air for the top (outer diameter, OD) and bottom (inner diameter, ID) walls of the combustor is not included in the total rig airflow. The total combustor rig airflow comprises only air that enters through the swirlers and air-cooled bulkhead, and through the quench/dilution/trim air holes in the OD and ID walls of the combustor rig. The JBTS facility provides separate control and metering of the airflow delivered to the combustor front-end (swirlers and bulkhead), top-wall

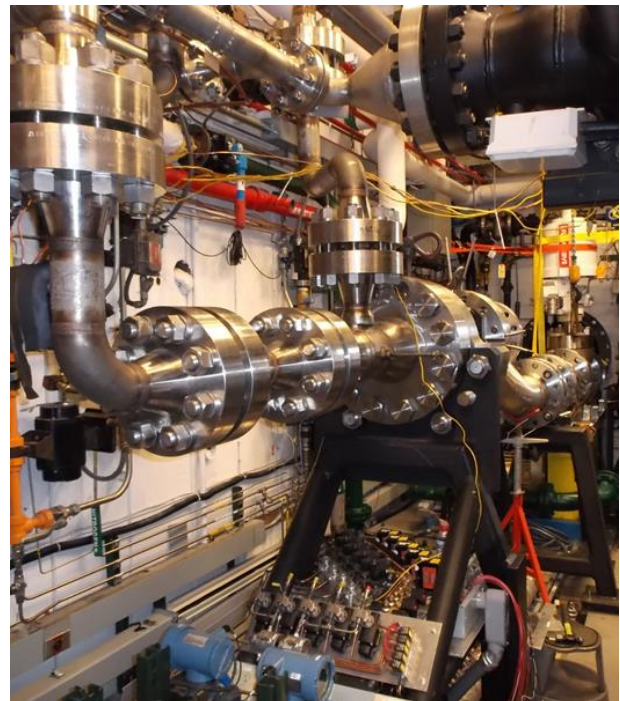


**FIGURE 4. High pressure single sector centerline in RTRC’s Jet Burner Test Stand.**

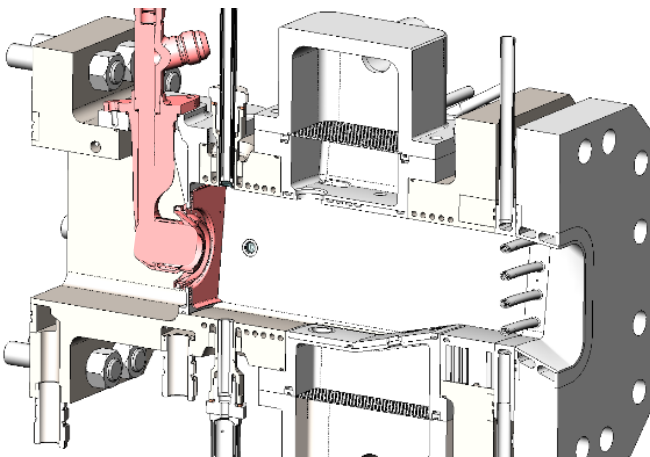


**FIGURE 5. FT4000 Single Nozzle Combustor Rig (SNR).**

(OD quench and dilution air holes), and bottom-wall (ID quench and dilution/trim air holes), enabling exact control of the airflow distribution to match the FT4000 engine combustor. The absence of liner cooling air does not measurably impact combustor performance, as the liner cooling air does not participate in the bulk combustion process, away from the walls, that is sampled by the emissions probes.

The single-sector combustor rig was designed to match the FT4000 engine combustor geometry as closely as possible in a water-cooled configuration that does not include the TALON combustor's double-wall liner panels and film-cooling features. Thus, the combustion-zone volumes (and corresponding residence times) and major aerodynamic features were retained, including engine-like fuel/air injection and staged-air addition at the quench, dilution, and trim air holes. To account for the lack of liner cooling air in the water-cooled rig, two different fuel-air ratio (FAR) levels were defined to match engine conditions: a high FAR matching the engine fuel nozzle local FAR, and a low FAR to match the engine front-end (before quench) combustor FAR. As noted earlier, CFD cases for the engine and rig were

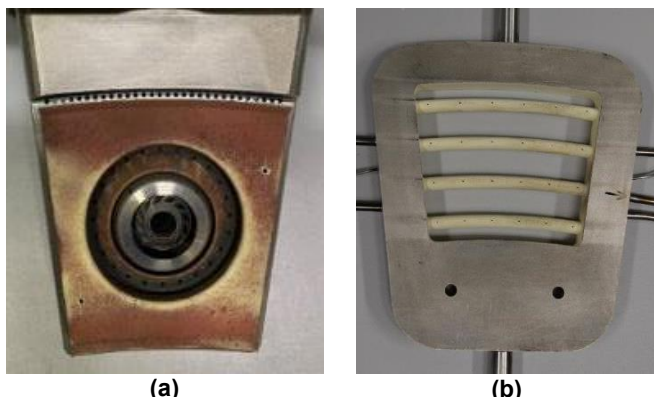


**FIGURE 6. Rig hardware: (a) FT4000 Fuel Nozzle Mixer and Bulkhead; (b) Emissions Sampling Rake.**

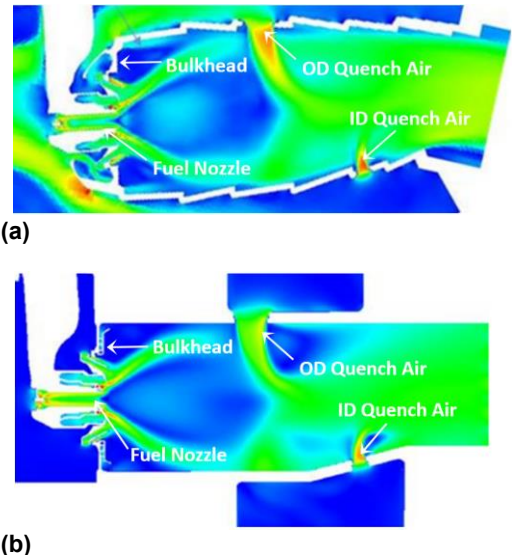


**FIGURE 7. CFD analysis of engine (a) and rig (b) combustor velocity flowfields.**

compared to confirm similar flow behavior in all combustion zones including the front-end flame-stabilization zone, air-jet penetrations, and aft burnout zone. A comparison of combustor flowfields obtained from CFD for the engine and rig are shown in Fig. 7 for a single cut plane. The velocity flowfield in the rig properly captures the front end flowfield setup by the fuel nozzle and the quench zone downstream. The results were used to finalize the rig design details to ensure the engine aerodynamics were properly replicated.

### 2.3 Experimental Setup

Figure 8 shows a flow schematic for the combustion rig testing reported here. Air is supplied through three separate circuits, each for i) bulkhead and fuel nozzle, ii) OD quench holes and iii) ID quench holes. Each circuit is pressurized by either a  $\sim 400$  psia (2750 kPa) air compressor system for medium pressure tests ( $P_3 < 300$  psi / 2000 kPa) or a  $\sim 1500$  psia (10300 kPa) diesel boost compressor system for high pressure tests ( $P_3 > 300$  psi / 2000 kPa). Independent 720 kW resistive air heaters heat the air for each circuit from ambient temperature to the desired combustor inlet temperature ( $T_3$ ), typically  $1075^{\circ}\text{F}$  (853K). All air flowrates are measured by choked sonic venturis. For the supply of fuels, high pressure natural gas is continuously supplied by an in-house boost compressor while hydrogen is delivered from maximum 1800 psia (12500 kPa) hydrogen trailers. The fuels are individually controlled and metered by regulators, on/off valves, control valves and Coriolis meters, and mixed approximately 30 ft (10 m) upstream of the rig. Unlike natural gas, the hydrogen supply line consists of high and low flow legs such that the combination of the two covers the wide range of hydrogen flow required in this study. The fuel mixture is heated by a steam heater up to  $\sim 220^{\circ}\text{F}$  (380K) before it is injected through the gaseous fuel passage of the nozzle.

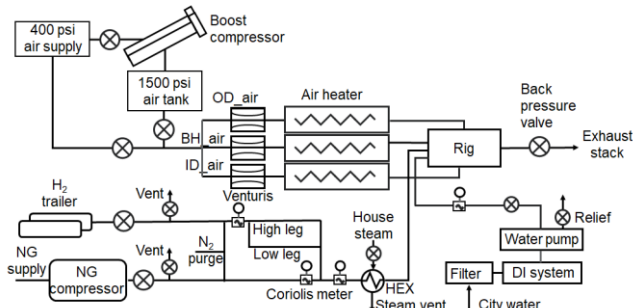


**FIGURE 8. Schematic of experimental setup.**

The FT4000 is a wet combustor, utilizing water injection through the nozzle passages for NOx control. A deionized (DI) water system, continuously operated with city water, feeds the water injection system. The deionized water is pumped up to ~900 psi (6000 kPa) by a ~6 gallons per minutes (1.35 m<sup>3</sup>/hr) capacity water pump before it is metered by Coriolis meters and injected to the water injection passages in the nozzle. A small portion of the deionized water is used to cool an optical probe for flame visualization, which will be described in the next section.

## 2.4 Measurement Techniques

The emission sampling system consists of an additively manufactured emission probe, pictured in Fig 6 (b). Four independently valved lines carry the sampled gas to independent analyzers for NO<sub>x</sub>, carbon monoxide (CO), carbon dioxide (CO<sub>2</sub>), oxygen (O<sub>2</sub>) and unburnt hydrocarbons (UHC) measurements. The emission probe samples post-combustion gas through four radially distributed rakes with six sampling holes at different circumferential locations of each radial position. Each radial sample is carried by heated sample lines and input to the analyzers as wet (NO<sub>x</sub>, O<sub>2</sub> and UHC) or semi-dry (CO and CO<sub>2</sub>) gas. The analyzer bench is composed of chemiluminescence NO<sub>x</sub>, non-dispersive infrared (NDIR) CO &

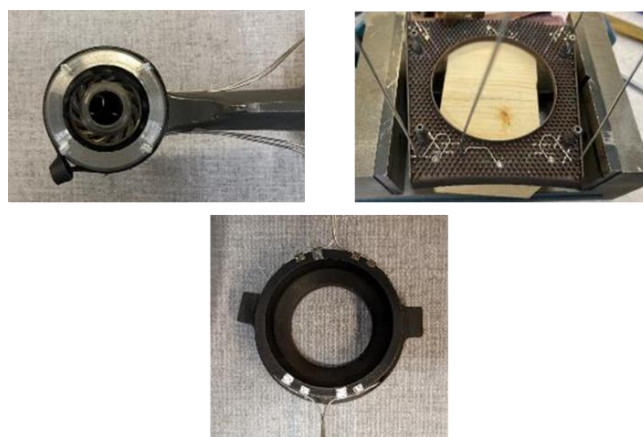


**FIGURE 9. Thermocouples installed on the fuel/air mixer, guide swirler and bulkhead hardware.**

CO<sub>2</sub>, paramagnetic O<sub>2</sub> and flame ionization detection UHC analyzers. Two analyzers are used for each species aiming for redundant measurements. All emission results reported in this study are from ganged measurements (sample streamed combined) for the entire radial and circumferential locations and post processed following SAE ARP 1533 standard [43]. An error propagation analysis based on a perturbation method was performed and the uncertainties for reported emissions results are approximately ±3% for NO<sub>x</sub>, ±1% for CO<sub>2</sub>, and ±1% for UHC measurements, respectively. Similarly, the uncertainty on percent hydrogen is on order of ±0.5%.

A ¼-inch (6mm) diameter rigid optical borescope was used for proof of light and visualization of flame location, flame shape and visible radiation from nozzle hot surfaces for health monitoring. The borescope features a 68° field of view and is housed in a water-cooled stainless-steel sheath with a fused silica window on the viewing end. Nitrogen is used for cooling and purging the combustion side of the window while cooling water flows between the borescope and window to cool the borescope optics. The scope is paired with a video rate (24-60 Hz) machine vision camera with no optical filter applied.

Numerous thermocouples (TCs) and pressure transducers were employed across the rig and facility. In addition, fourteen 0.007-in. (0.18 mm) K-type TCs with 0.040-in. (1mm) sheath were instrumented across the nozzle end cap, guide swirler and bulkhead as shown in Fig. 9. In conjunction with real time imaging from the borescope, these fast response TCs were used to monitor and detect the surface temperature increase caused by changes in flame location or flame anchoring in their vicinities. It is noted that the combustor exit temperature (T4) reported in this study is not directly measured, but rather is derived from equilibrium calculations based on rig inlet conditions, as detailed in the next section.

**TABLE 1. Summary of test periods for FT4000 fuel nozzle evaluation in Single Nozzle Rig with test objectives and %H<sub>2</sub> by volume achieved.**

Day	Test Objectives	Hydrogen vol%									
		0	10	30	40	50	60	70	80	90	100
1	Rig baseline/validation on NG	█									
2	Impact of hydrogen up to 30%		█								
3	Impact of water injection			█	█						
4	Impact of pressure				█	█	█	█	█	█	
5	Impact of higher hydrogen %								█	█	█

**TABLE 2. Summary of test periods for FT4000 fuel nozzle evaluation with conditions achieved.**

Test Period	Pressure (psia/kPa)	Temperature (deg F/deg K)	H2 Vol%	WFR/WFR <sub>nominal</sub>
1	300/2070	1075/853	0	0.9 to 1.25
2	245/1690	1075/853	0, 10, 30	1.0 to 1.3
3	245/1690	1075/853	30, 40	1.0 to 1.3
4	395/2720	1060/844	0, 10, 30-74	1.0 to 1.4
5	275/1900	1075/853	50-100	1.3 to 3.1

## 2.5 Test Conditions

Table 1 highlights the high-level objective of each test period with the progression of hydrogen volume percentage in the fuel mixture. Table 2 contains more detailed rig conditions, scaled from engine conditions, studied for each test period. During the first test period, 100% natural gas was used to establish baseline emissions data in the rig at a moderate pressure of 300 psia (2068 kPa). Water fuel ratio (WFR) was varied above and below the nominal engine operating point ( $WFR_{nominal}$ ). Rig emissions and performance was compared to previously obtained full annular rig and engine data to validate the emissions, as detailed in the results section. In the second test period, hydrogen was blended with natural gas, ramping up to 30% by volume at both high and low fuel-air ratio (FAR) levels. The third test period focused on the method of water injection through the fuel nozzle, with 30% and 40% hydrogen evaluated in the rig, again at two different FAR levels. For these tests, FAR is defined as the total fuel mass flowrate (natural gas plus hydrogen) divided by the total air flowrate (front-end plus quench air).

For the fourth test period, the impact of pressure on NOx and flame position was evaluated. The boost compressors were utilized to increase the supply pressure, up to an inlet pressure of 395 psia (2723 kPa). Hydrogen percentage was increased in roughly 10% increments, up to 75% by volume. Water fuel ratio (WFR), normalized by the baseline level, during the first four test periods ranged from 0.9 to 1.4. The nominal or baseline WFR level is defined as the reference WFR of the engine during baseline operation with natural gas.

The primary objective on the last test period was to determine the safe operating limit for the fuel nozzle/combustor with hydrogen. The percent hydrogen was increased while holding the calculated combustor exit temperature,  $T_4$ , constant. As hydrogen flow was increased, natural gas flow was reduced with a constant airflow. Operation on 100% hydrogen with water injection was achieved. Water fuel ratio (WFR), normalized by the baseline level, during the final test ranged from 1.3 to 3.1. Detailed results will be described in the following section.

## 3. RESULTS AND DISCUSSION

### 3.1 Natural Gas Only Baseline/Validation

The rig was first characterized by running on natural gas and water at near full baseload conditions. NOx emissions for the natural gas baseline tests are shown in Fig. 10, along with reference data from previous FT4000 full annular combustor tests and two FT4000 engine tests. As can be seen in the figure, the single nozzle rig NOx emissions follow the same trends as the annular combustor and engine data for natural gas operation. Baseline NOx emissions at the nominal water-fuel ratio (WFR) align with prior experience. It is also shown that NOx emissions are dominated by water-fuel ratio in this wet system.

### 3.2 Hydrogen/Natural Gas Blends and 100% Hydrogen

Following the baseline natural gas validation tests, hydrogen was introduced into the natural gas in increasing amounts.

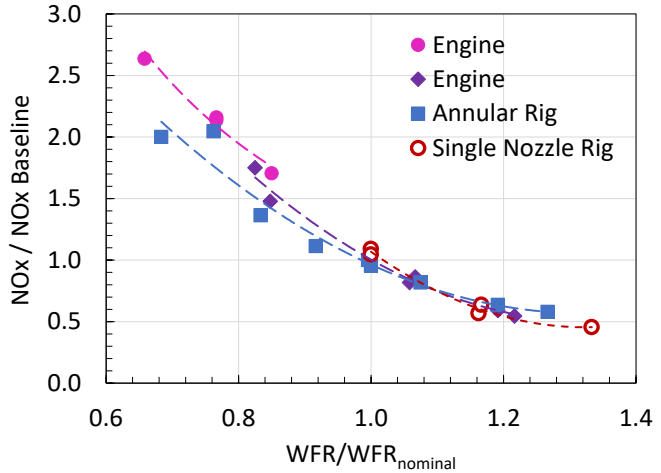


FIGURE 10. Validation of rig on natural gas.  $P_3=394$  psia,  $T_3=1060^{\circ}\text{F}$ .

During these tests, considerable attention was paid to live video of the flame location from the imaging probes and fuel nozzle temperatures from nozzle-mounted thermocouples (Fig. 9). Over a period of five test periods, confidence was gained that the fuel nozzle could support higher levels of hydrogen without experiencing damaging flashback or flameholding.

NOx emission results as a function of percent hydrogen from 0 to 75% are shown in Fig. 11 with FAR held constant as the WFR was varied. The NOx values reported are corrected using the correction provided in Ref. [44] for hydrocarbon blends. This correction accounts for biases in comparing traditional hydrocarbon fuels with hydrogen blends due to the increased water production and reduced  $\text{O}_2$  consumption that biases the dry and 15%  $\text{O}_2$  correction.

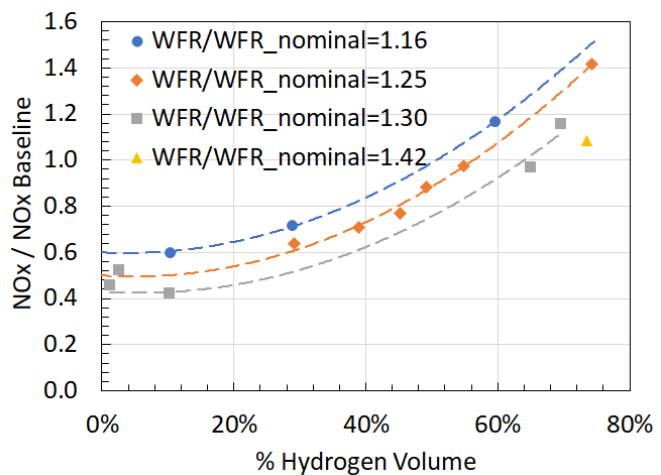
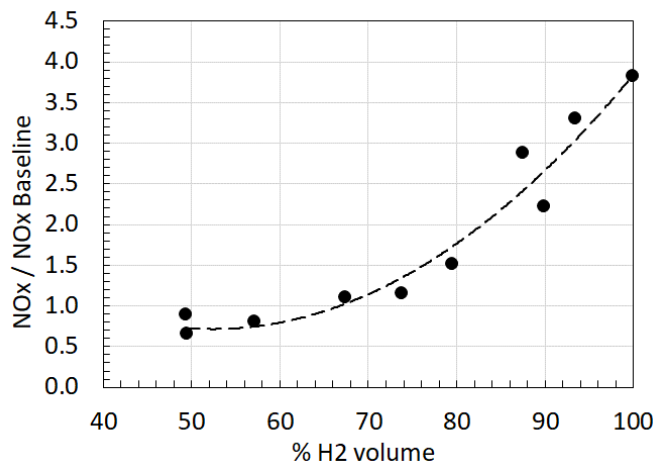
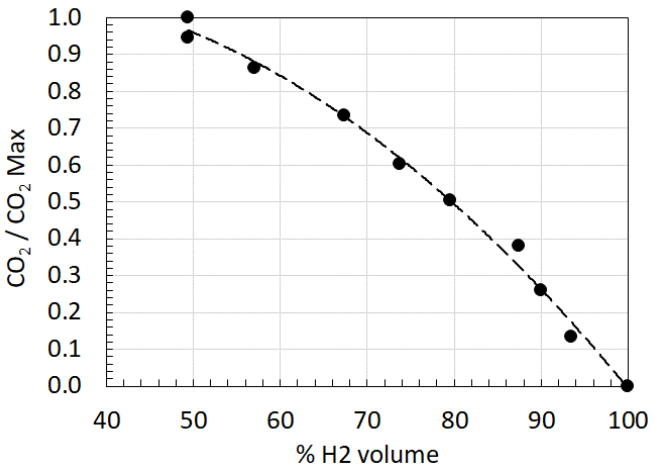


FIGURE 11. NOx emissions results for bill-of-materials fuel nozzle with FAR held constant and percent hydrogen varying from 0 to 75%.  $T_4$  is increasing with  $\% \text{H}_2$ .  $P_3=395$  psia,  $T_3=1060^{\circ}\text{F}$ .



(a) NOx emissions



(b) CO<sub>2</sub> Emissions

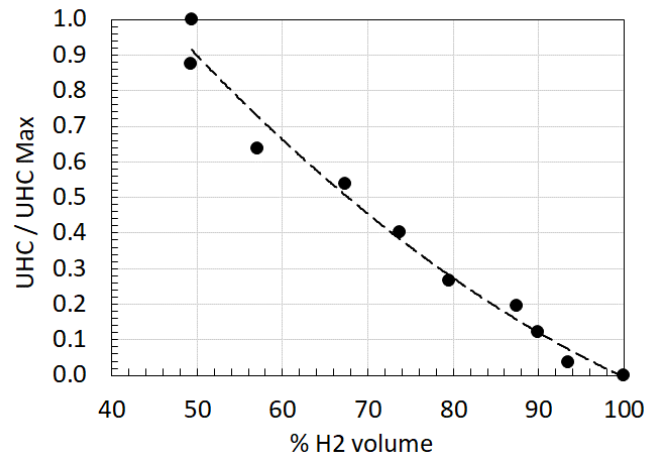


FIGURE 12. Emissions results as a function of percent hydrogen with WFR and T4 held constant: (a) NOx emissions; (b) normalized CO<sub>2</sub> emissions; (c) normalized unburned hydrocarbons. P3=275 psia and T3=1075°F.

In Fig. 11, NOx is shown to increase with percent hydrogen for all WFR's tested. This is primarily due to the higher flame temperature of hydrogen compared to natural gas at an equivalent fuel-air ratio. By holding fuel-air constant while increasing percent hydrogen, the T4 temperature increases by approximately 10% from 0 to 75% hydrogen, thus yielding higher NOx production. The results also show that increasing WFR results in lower NOx for all hydrogen levels. Near baseline NOx level was achieved at 75% hydrogen with approximately 40% higher water-to-fuel ratio relative to the natural gas baseline.

During these tests, a hot spot was observed on the fuel nozzle endcap above 40% hydrogen. This hot spot was visible in the thermocouple data as well as with the optical imaging probe. Changes were made to the water injection distribution within the fuel nozzle to maintain acceptable metal temperatures. Post test inspection of the fuel nozzle between test periods showed no damage to the fuel nozzle. Therefore, it was decided to continue to a final limit test to determine the operability/durability limit with high levels of hydrogen. For the final limit test, the test matrix was adjusted by reducing FAR to hold T4 constant while

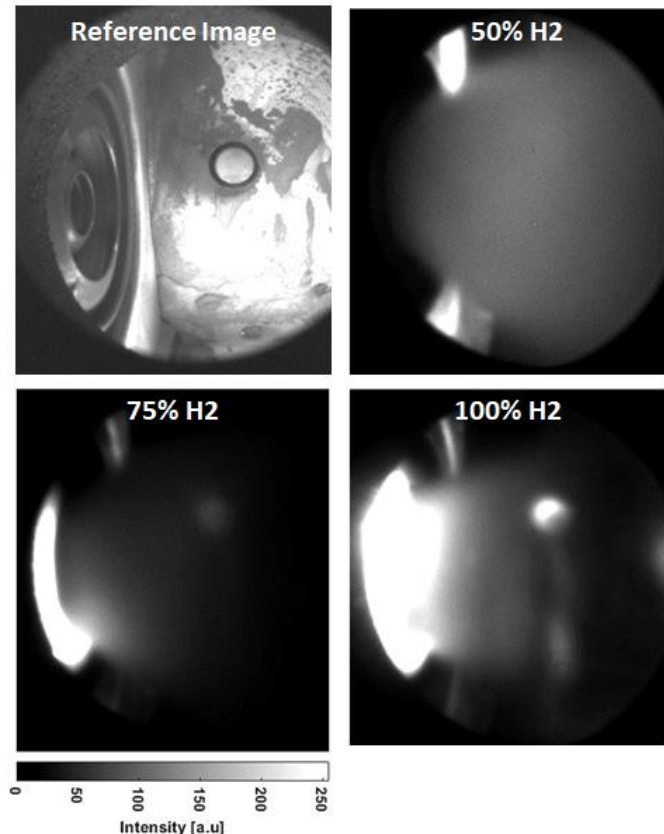
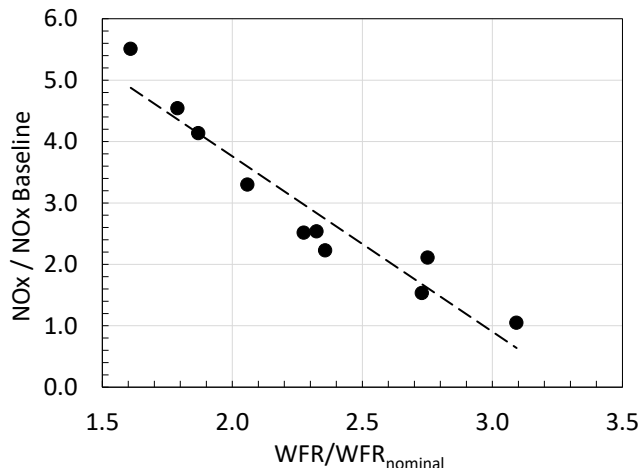


FIGURE 13. Representative instantaneous images of flame luminosity for 50% H<sub>2</sub>/NG, 75% H<sub>2</sub>/NG and 100% H<sub>2</sub> obtained from imaging probe viewing into combustor in vicinity of the fuel nozzle. Fuel nozzle is visible in reference image top left.



**FIGURE 14. NOx emissions versus normalized WFR for 100% hydrogen. FAR has been held constant, thus T4 is decreasing slightly as WFR increases. P3=275 psia, T3=1075 °F.**

increasing the percentage of hydrogen. FAR was reduced by 58% from 50 to 100% hydrogen.

The final limit test proceeded from 50% hydrogen and advanced up to 100% hydrogen while holding T4 constant (corresponding to high power baseload condition) with WFR nearly constant between  $WFR/WFR_{nominal} \sim 1.4-1.8$ . Operation of the FT4000 fuel nozzle up to 100% hydrogen was achieved with optimized water injection. Emissions results for NOx, carbon dioxide ( $CO_2$ ) and unburned hydrocarbons (UHC) are shown in Fig. 12. The results show NOx emissions increasing as percent hydrogen is increased while holding T4 constant, with nearly constant WFR. For all cases, combustion efficiency was near or above 99%. Carbon dioxide emissions and unburned hydrocarbons are shown to decrease to zero as 100% hydrogen is reached.



**FIGURE 15. Image of fuel nozzle and guide swirler condition post-test. Minor distress is noted on the fuel nozzle endcap, while no distress is evident on the internal fuel/air mixer. The endcap distress is believed to have occurred during a short transient when water was reduced significantly while operating on 100% hydrogen.**

Representative visual (unfiltered, instantaneous) images from the optical imaging probe for operation with 50%, 75% and 100% hydrogen are shown in Fig. 13. For 50% hydrogen, the bright spots in the image correspond to flame reflection from the bulkhead panel. At 75% and 100% hydrogen, there is significant light emission noted from the fuel nozzle region, suggesting the flame is shifting farther upstream and closer to the nozzle under these conditions. Even though the flame moved further forward, thermocouple metal temperatures remained acceptable without any signs of damage or flameholding inside the fuel nozzle.

While operating on 100% hydrogen, additional mapping of the effect of WFR was conducted while holding fuel and air flows constant. Fig. 14 shows that for 100% hydrogen and constant FAR, increasing the WFR reduces NOx in an approximately linear fashion. For this test sequence, there is a reduction in T4 of approximately 10% as WFR is increased while holding fuel and air flows constant. A WFR increase of 3x is needed to reduce the NOx emissions to baseline (natural gas) levels. Due to the lower mass flow of hydrogen needed to provide comparable power level to the natural gas baseline, the absolute water flowrate is only ~30% higher than the baseline case.

For all conditions tested, stable flame anchoring was observed, with no indication of lean blow out (LBO) or instability with all water levels tested. During testing, unsteady pressure in the combustor was also monitored. A limited number of tests were conducted with a choked acoustic boundary at the exit of the combustor. The remainder of the testing was conducted with an unchoked combustor exit. For all conditions tested, while operating with hydrogen/natural gas blends and pure hydrogen, unsteady pressure amplitudes were in-line with or lower than the natural gas baseline.

A photograph of the fuel nozzle taken post-test is shown in Fig. 15. The internal fuel/air mixer is fully intact with no signs of distress. The nozzle endcap shows some signs of minor distress. This distress is believed to have occurred during a transient when water flow was momentarily reduced significantly while operating on 100% hydrogen. This is supported by optical images and thermocouple data which show increase in fuel nozzle endcap temperatures during this excursion.

Future efforts will focus on improving the robustness of the fuel nozzle and guide swirler design for high hydrogen and reduce the dependency on water injection to keep the nozzle cool.

#### 4. CONCLUSION

High-pressure single-sector combustor testing of an FT4000 dual-fuel nozzle has demonstrated successful operation on 100% hydrogen fuel with water injection providing robust operation and nitrogen oxide (NOx) emissions meeting target values.

The single-sector FT4000 combustor rig performance was first validated for purely natural gas operation at simulated baseload operating conditions (rig pressure and temperature near 400 psi and 1050°F) and was then used to test hydrogen blended with natural gas at 10, 30, 40, 50, 75, and 100% hydrogen by

volume. Hardware temperatures and flame position were monitored optically and with thermocouples, showing safe operation throughout the testing.

Results from this study have cleared the current production FT4000 engines with dual fuel nozzles to operate at baseload power on hydrogen/natural gas blends with water injection.

## ACKNOWLEDGEMENTS

This material is based upon work supported by the Department of Energy under Award Number DE-FE0032171. The authors would like to acknowledge the financial support provided by Mitsubishi Power Aero in the design, fabrication, assembly and initial planning and testing of the single sector rig.

**Disclaimer:** This report was prepared as an account of work sponsored by an agency of the United States Government. Neither the United States Government nor any agency thereof, nor any of their employees, makes any warranty, express or implied, or assumes any legal liability or responsibility for the accuracy, completeness, or usefulness of any information, apparatus, product, or process disclosed, or represents that its use would not infringe privately owned rights. Reference herein to any specific commercial product, process, or service by trade name, trademark, manufacturer, or otherwise does not necessarily constitute or imply its endorsement, recommendation, or favoring by the United States Government or any agency thereof. The views and opinions of authors expressed herein do not necessarily state or reflect those of the United States Government or any agency thereof.

FT4000 and SWIFTPAC are registered trademarks of Mitsubishi Power Aero LLC, used with permission.

## REFERENCES

- [1] FT4000® SWIFTPAC® Gas Turbine Package fact sheet, available at [mhi.com](http://mhi.com) (2023), [Mitsubishi Power | FT4000® SWIFTPAC® \(mhi.com\)](http://mhi.com)
- [2] R.G. McKinney, D. Sepulveda, W. Sowa, A.K. Cheung (2007), “The Pratt & Whitney TALON X Low Emissions Combustor: Revolutionary Results with Evolutionary Technology,” Paper No. AIAA-2007-386, 45th AIAA Aerospace Sciences Meeting, Reno, Nevada, 8-11 January 2007.
- [3] Samuels, S. (2006), “Rich Burn, Quick Mix, Lean Burn (RQL) Combustor,” Chapter 3.2.1.3 in *The Gas Turbine Handbook*, U.S. Department of Energy, Publication No. DOE/NETL-2006/1230, <http://www.netl.doe.gov/technologies/coalpower/turbines/refshlf/handbook/TableofContents.html>.
- [4] J.N. Sivo and D.B. Fenn (1956), “Performance of a Short Combustor at High Altitudes Using Hydrogen Fuel,” NACA Research Memorandum No. RM-E56D24.
- [5] I. L. Drell and F. E. Belles (1958), “Survey of Hydrogen Combustion Properties,” NACA Report 1383.
- [6] P.M. Ordin (1997). “Safety Standard for Hydrogen and Hydrogen Systems.” NASA Safety Standard NSS.1740.16.
- [7] A Contreras, S. Yigit, K. Ozay, and T.N. Veziroglu (1997), “Hydrogen as Aviation Fuel: A Comparison with Hydrocarbon Fuels,” *Int. J. Hydrogen Energy*, Vol. 22, No. 10/11, pp. 1053-1060.
- [8] Y.C. Lin, P. Jansohn, K. Boulouchos (2014), “Turbulent flame speed for hydrogen-rich fuel gases at gas turbine relevant conditions,” *Int. J. Hydrogen Energy*, Vol. 39, pp. 20242-20254.
- [9] C.B. Meher-Homji and E. Prisell (2000), “Pioneering Turbojet Developments of Dr. Hans Von Ohain – From the HeS1 to the HeS011,” *Journal of Engineering for Gas Turbines and Power*, Vol. 122, p. 191.
- [10] L. Langston (2019), “Hydrogen Fueled Gas Turbines,” *Mechanical Engineering magazine*, Vol. 141, 6 March 2019, 10.1115/1.2019-MAR-6.
- [11] J.L. Sloop (1978), “Liquid hydrogen as a propulsion fuel, 1945-1959,” NASA Report No. NASA-SP-4404.
- [12] W.D. Rayle, R.E. Jones, and R. Friedman (1957), “Experimental Evaluation of ‘Swirl-Can’ Elements for Hydrogen-Fuel Combustor,” NACA Research Memorandum No. NACA-RM-E57C18 (declassified 1971).
- [13] C.T. Norgren and R.D. Ingebo (1974), “Emissions of Nitrogen Oxides from An Experimental Hydrogen-Fueled Gas Turbine Combustor,” NASA Technical Memorandum No. NASA-TM-X-2997.
- [14] D.N. Anderson (1976), “Emissions of Oxides of Nitrogen from An Experimental Premixed-Hydrogen Burner,” NASA Technical Memorandum No. NASA-TM-X-3393.
- [15] J. Brand, S. Sampath, F. Shum, R. Bayt, and J. Cohen (2003), “Potential Use of Hydrogen In Air Propulsion,” AIAA Paper No. AIAA-2003-2879, July 2003, Dayton, Ohio.
- [16] J. Ziemann, F. Shum, M. Moore, D. Kluyskens, D. Thomaier, N. Zarzalis, and H. Eberius (1998), “Low-NOx Combustors for Hydrogen Fueled Aero Engine,” *Int. J. Hydrogen Energy*, Vol. 23, pp. 281-288.
- [17] F. Shum, M. Moore, J. Cohen, T. Rosfjord, H. Eberius, J. Ziemann, D. Thomaier, B. Simon (1996), “Potential Use of Hydrogen in Air Propulsion,” Final Report to Hydro-Quebec Contract No. 16233-92-ERE-015-00 and to European Union Contract No. 4541-91-11-EL-ISP-PC, December 1996.
- [18] C.J. Marek, T.D. Smith, and K. Kundu (2005), “Low Emission Hydrogen Combustors for Gas Turbines Using Lean Direct Injection,” AIAA Paper No. AIAA-2005-3776, July 2005, Tucson, Arizona.
- [19] G. Andrews, M. Altaher, and H. Li (2012), “Hydrogen Combustion at High Combustor Airflow using an Impinging Jet

Flame Stabiliser with no Flashback and Low-NOx,” ASME Paper No. GT2012-70052, June 2012, Copenhagen, Denmark.

[20] W. York, W. Ziminsky, and E. Yilmaz (2012), “Development and Testing of a Low NOx Hydrogen Combustion System for Heavy Duty Gas Turbines,” ASME Paper No. GT-2012-69913.

[21] W. York, M. Hughes, J. Berry, T. Russell, Y.C. Lau, S. Liu, M.D. Arnett, A. Peck, N. Tralshawala, J. Weber, M., M. Iduate, J. Kittleson, A. Garcia-Crespo, J. Delvaux, F. Casanova, B. Lacy, B. Brzek, C. Wolfe, P. Palafox, B. Ding, B. Badding, D. McDuffie, and C. Zemsky (2015), “Advanced IGCC/Hydrogen Gas Turbine Development,” Final Technical Report to U.S. DOE for Cooperative Agreement No. DE-FC26-05NT42643.

[22] H. Funke, J. Keinz, W. Kusterer, A.H. Ayed, M. Kazari, J. Kitajima, A. Horikawa, K. Okada (2017), “Development and Testing of a Low NOx Micromix Combustion Chamber for Industrial Turbines,” International Journal of Gas Turbine, Propulsion and Power Systems, Vol. 9, No. 1.

[23] H. Funke, N. Beckmann, S. Abanteriba (2019), “An overview on dry low NOx micromix combustor development for hydrogen-rich gas turbine applications,” Int J Hydrogen Energy, Vol. 44, pp. 6978-6990.

[24] B.M. Webb, J. Harper, R. Steele, D.R. Noble, B. Emerson, D. Wu, and T. Lieuwen (2023), “Second Edition: Assessment of Current Capabilities and Near-Term Availability of Hydrogen-Fired Gas Turbines Considering a Low-Carbon Future,” ASME Paper No. GT2023-103962, June 2023, Boston, Massachusetts.

[25] M.J. Hughes, J.D. Berry, W. Zhao, B. Crawley, T. Onyima, H. Feiz, E. Paasche, L. Cretegny, S. Hong, T. Genova, and H. Bower (2023), “DLN Evo Combustion Technology Development for a High-Hydrogen Flexible F-Class Retrofit,” ASME Paper No. GT2023-101797, June 2023, Boston, Massachusetts.

[26] D. Pennell, L. Tay-Wo-Chong, R. Smith, P.S. Sanchez, A. and Ciani (2023), “GT36 First Stage Development Enabling Load and Fuel (H2) Flexibility with Low Emissions,” ASME Paper No. GT2023-103568, June 2023, Boston, Massachusetts.

[27] J. Harper, S. Cloyd, T. Pigon, B. Thomas, J. Wilson, E. Johnson, and D.R. Noble (2023), “Hydrogen Co-firing Demonstration at Georgia Power’s Plant McDonough: M501G Gas Turbine,” ASME Paper No. GT2023-102660, June 2023, Boston, Massachusetts.

[28] R.C. Steele, T.D. Martz, A. Ettlinger, T. Zandes, M.J. Alexander, B.K. Hockman, and J. Goldmeer (2023), “Hydrogen Co-firing Demonstration at New York Power authority Brentwood Site: GE LM6000 Gas Turbine,” ASME Paper No. GT2023-101283, June 2023, Boston, Massachusetts.

[29] I.G. Escudero, B. Tran, M. Overbaugh, V. McDonell, B. Williams, P. Buelow, J. Ryon, and O. DeBeni (2023), “Adaptation of Aeroengine Micromixing Injectors for Lean Direct Injection of Hydrogen and Hydrogen/Natural Gas Blends,” ASME Paper No. GT2023-101577, June 2023, Boston, Massachusetts.

[30] B. Lewis and G. von Elbe (1987), “Combustion, Flames, and Explosions of Gases,” Third Edition, Academic Press, Inc., New York, NY.

[31] M. Fukuda, K. Korematsu, M. Sakamoto (1981), “On Quenching Distance of Mixtures of Methane and Hydrogen in Air,” Bulletin of the Japan Society of Mechanical Engineers (JSME), Vol. 24, No. 193.

[32] R. Jones and N. Shilling (2003), “IGCC Gas Turbines for Refinery Applications,” GE Report No. GER-4219.

[33] R. Jones, J. Goldmeer, B. Monetti (2011), “Address Gas Turbine Fuel Flexibility,” GE Report No. GER-4601b.

[34] J. Wu, P. Brown, I. Diakunchak, A. Gulati, M. Lenze, and B. Koestlin (2007), “Advanced Gas Turbine Combustion System Development for High Hydrogen Fuels,” ASME Paper No. GT2007-28337, May 2007, Montreal, Canada.

[35] W. Laster and E. Anoshkina (2007), “Catalytic Combustor for Fuel-Flexible Turbine,” Siemens Power Generation Final Report to U.S. DOE for Contract No. DE0FC26-03NT41891.

[36] Smith, L.L. (2004). “Ultra Low NOx Catalytic Combustion for IGCC Power Plants.” Final Report to DOE for Phase I of DOE Contract No. DE-FC26-03NT41721.

[37] Smith, L.L., Karim, H., Castaldi, M.J., Etemad, S., & Pfefferle, W.C. (2006). “Rich-Catalytic Lean-Burn Combustion for Fuel-Flexible Operation with Ultra-Low Emissions.” *Catalysis Today*, 117, 438-446.

[38] Smith, L.L., Karim, H., Etemad, S., & Pfefferle, W.C. (2006). “Fuel-Rich Catalytic Combustion.” Chapter 3.2.2.1 in *The Gas Turbine Handbook*, U.S. Department of Energy, Publication No. DOE/NETL-2006/1230, <https://www.netl.doe.gov/sites/default/files/gas-turbine-handbook/3-2-2-1.pdf>.

[39] Modern Power Systems magazine (2021), “Gas turbines in the US are being prepped for a hydrogen-fuelled future,” 6 January 2021, <https://www.nsenergybusiness.com/features/gas-turbines-hydrogen-us/>.

[40] ETN Global fact sheet, <https://etn.global/gas-turbine-products/ft4000-swiftpac-gas-turbine-package/>.

[41] ICAO Aircraft Engine Emissions Databank (06/2023) <https://www.easa.europa.eu/en/domains/environment/icao-aircraft-engine-emissions-databank>

[42] Snyder, T.S., Rosfjord, T.J., McVey, J.B. and Chiapetta, L.M., "Comparison of Liquid Fuel/Air Mixing and NOx Emissions for a Tangential Entry Nozzle," ASME Paper 94-GT-283, 1994.

[43] Procedure for the Analysis and Evaluation of Gaseous Emissions from Aircraft Engines, Aerospace Recommended Practice ARP1533 Rev C, SAE International, April 13, 2016.  
<https://www.sae.org/standards/content/arp1533c/>

[44] Douglas, C. M. , Emerson, B. L. , Lieuwen, T. C. , Martz, T., Steele, R. , and Noble, B., 2022, "NOx Emissions From Hydrogen-Methane Fuel Blends," Georgia Institute of Technology, Strategic Energy Institute, Atlanta, GA, Report.

[https://research.gatech.edu/sites/default/files/inline-files/gt\\_epri\\_nox\\_emission\\_h2\\_short\\_paper.pdf](https://research.gatech.edu/sites/default/files/inline-files/gt_epri_nox_emission_h2_short_paper.pdf)